this problem one can use the nonequilibrium Green's function formalism developed by Kadanoff and Baym.[16] One has to calculate the time change of the total momentum of the Fermi system for $U(\vec{r}, t)$ varying slowly in time, i.e., for a situation close to local thermodynamic equilibrium. We have been unsuccessful in carrying out this program even for a weakly interacting Fermi gas.

The essential approximation which leads from the above-mentioned microscopic approach to Landau's transport equation used in Secs. I–III is the assumption that all quantities vary slowly in space.[16] Although this is certainly not true for a hard-sphere impurity, it seems a good approximation if the impurity is large enough.

In closing we would like to mention the work of Gould and Ma[10] who calculate the mobility in a weakly interacting Fermi gas. Their basic mobility formula is obtained by using second-order perturbation theory in the time-dependent part of the impurity potential. The treatment takes into account the density oscillations in the vicinity of the static impurity but does not allow for density changes caused by the movement of the impurity. As pointed out before[11] their final result arises as a consequence of an inconsistent expansion. Without this expansion it can be shown that the new contributions vanish for a large impurity. Also the authors of Ref. 10 treat the fermion interaction to first order, thereby neglecting the effects of quasiparticle collisions.

ACKNOWLEDGMENTS

The author wishes to thank Professor D. C. Langreth and Professor M. J. Stephen for very helpful discussions.

---

*Work supported by the National Science Foundation.

[1]J. C. Wheatley, Phys. Rev. 165, 304 (1968); in *Quantum Fluids*, edited by D. F. Brewer (North-Holland, Amsterdam, 1966), p. 183.

[2]A. A. Abrikosov and I. M. Khalatnikov, Rept. Progr. Phys. (Kyoto) 22, 329 (1959).

[3]K. S. Dy and C. J. Pethick, Phys. Rev. 185, 373 (1969).

[4]Ryuzo Abe and Ko Aizu, Phys. Rev. 123, 10 (1961).

[5]R. C. Clark, Proc. Phys. Soc. (London) 82, 785 (1963).

[6]G. T. Schappert, Phys. Rev. 168, 162 (1968).

[7]H. Winter, Z. Physik 221, 186 (1969).

[8]B. D. Josephson and J. Lekner, Phys. Rev. Letters 23, 111 (1969).

[9]H. Ted Davis and R. Dagonnier, J. Chem. Phys. 44, 4030 (1966).

[10]H. Gould and S. Ma, Phys. Rev. Letters 21, 1379 (1969); Phys. Rev. 183, 338 (1969).

[11]Lorenz Kramer, Phys. Rev. A 1, 1517 (1970), hereafter referred to as I.

[12]A. C. Anderson, M. Kuchnir, and J. C. Wheatley, Phys. Rev. 168, 261 (1968).

[13]M. Kuchnir, Pat R. Roach, and J. B. Ketterson Phys. Rev. A 2, 262 (1970).

[14]L. D. Landau, Zh. Eksperim. i Teor. Fiz. 30, 1058 (1956)[Soviet Phys. JETP 3, 920 (1957)]; 32, 59 (1957) [5, 101 (1957)].

[15]D. Pines and P. Nozières, *The Theory of Quantum Fluids* (Benjamin, New York, 1966), Vol. I, Chap. 1.

[16]L. P. Kadanoff and G. Baym, *Quantum Statistical Mechanics* (Benjamin, New York, 1962).

PHYSICAL REVIEW A VOLUME 2, NUMBER 5 NOVEMBER 1970

Low-Temperature Mobility of Trapped Ions in Rotating He II†

Alexander L. Fetter* and Ienari Iguchi
Institute of Theoretical Physics, Department of Physics, Stanford University, Stanford, California 94305

(Received 22 May 1970)

A classical vortex with a movable impurity in its core is used to study the interaction of vortex waves with a trapped ion in rotating He II. The reflection probability is evaluated in the long- and short-wavelength limits. An approximate interpolation formula allows a calculation of the low-temperature mobility of an ion along the vortex axis.

I. INTRODUCTION

The mobility of a trapped ion moving along a vortex line in He II is smaller than that of a free ion.[1,2] This result is of great interest, for it is one of the few experiments that can provide information about the vortex core. At least three processes can account for the added resistance to the motion of the ion along the vortex line: frictional drag arising from trapped rotons,[3] scattering of quanta of vortex waves,[2] and creation of additional vortex waves. The first is important at higher temperatures ($T \gtrsim 1$ °K) and will not be considered here. Douglass[2] treated the second mechanism (scattering of vortex waves), using an approximate matching procedure at the surface of the ion. As an improved model for the true quantum system, we here study the classical scattering of vortex waves by a movable impurity of size $\approx A$ located in the vortex core. The treatment is similar to that of Levine[4] and Fetter[5] for surface waves on an infinite sea. In Sec. II, the scattering problem is formulated as a linear integral equation. The long- and short-wavelength solutions are obtained explicitly (Sec. III), allowing an approximate interpolation formula valid for all wavelengths. Section IV contains a discussion of our numerical results.

II. FORMULATION OF PROBLEM

The velocity field of an incompressible irrotational fluid satisfies[6]

$$\vec{v} = -\vec{\nabla}\Phi, \tag{1}$$

$$\nabla^2\Phi = 0. \tag{2}$$

Consider an infinite straight vortex with a hollow core of radius a surrounded by circulating fluid with density ρ_l. In equilibrium, the pressure $p_0(r)$ is given by Bernoulli's equation

$$\frac{p_0(r)}{\rho_l} + \tfrac{1}{2}[v_0(r)]^2 = \frac{1}{2}\left(\frac{\bar{\kappa}}{2\pi a}\right)^2, \tag{3}$$

where $\bar{\kappa}$ is the circulation about the vortex and $\vec{v}_0 = (\bar{\kappa}/2\pi r)\hat{\varphi}$ is the velocity field. Here $\vec{r} = (r, \varphi)$ is a two-dimensional radial vector perpendicular to the vortex axis.

We now disturb the inner surface of the core and examine the resulting small-amplitude oscillations when Φ_0 and $\vec{v}_0$ are modified by adding small perturbations Φ' and $\vec{v}'$. Bernoulli's equation becomes

$$\frac{p(r)}{\rho_l} + \tfrac{1}{2}(\vec{v}_0 + \vec{v}')^2 - \frac{\partial\Phi'}{\partial t} = \frac{1}{2}\left(\frac{\bar{\kappa}}{2\pi a}\right)^2, \tag{4}$$

which yields the total pressure $p(r)$ in the perturbed state

$$\frac{p(r)}{\rho_l} = \frac{1}{2}\left(\frac{\bar{\kappa}}{2\pi}\right)^2\left(\frac{1}{a^2} - \frac{1}{r^2}\right) + \frac{\bar{\kappa}}{2\pi r^2}\frac{\partial\Phi'}{\partial\varphi} + \frac{\partial\Phi'}{\partial t} \; . \tag{5}$$

Although Φ' can be a general function of the time, we consider only harmonic motion $e^{-i\omega t}$. If Φ' is assumed to take the form

$$\Phi'(\vec{r}, z, t) = f_l(r)\exp(il\varphi + ikz - i\omega t),$$

a straight-forward calculation[2,7] gives the dispersion relation

$$\omega = \Omega\left\{ l \pm \left[-\frac{kaK_l'(ka)}{K_l(ka)} \right]^{1/2} \right\}, \tag{6}$$

where $\Omega \equiv \bar{\kappa}/2\pi a^2$ and K_l is the Bessel function of imaginary argument that vanishes at infinity.[8] Only the modes $l = \pm 1$ are thermally excited in He II,[7] and, for definiteness, we take $l = -1$. With these assumptions, Eq. (5) can be written

$$\frac{p(r)}{\rho_l} = \frac{\bar{\kappa}^2}{8\pi^2}\left(\frac{1}{a^2} - \frac{1}{r^2}\right) - i\left(\frac{\bar{\kappa}}{2\pi r^2} + \omega\right)\Phi'. \tag{7}$$

We now turn to the more interesting case of an ion or impurity placed in the vortex core. For simplicity, this object will be approximated as a cylinder of radius a, length $2A$, and mass M, placed in contact with the cylindrical free surface of the liquid (Fig. 1). In equilibrium, the surface of the cylinder is given by the equation $r = a$. When vortex waves are present, the cylinder will be displaced harmonically, and the corresponding equation for its surface becomes

$$r = a + \epsilon_0 e^{-i\varphi}e^{-i\omega t} + \epsilon_1 z e^{-i\varphi}e^{-i\omega t}, \tag{8}$$

where ϵ_0 and ϵ_1 are infinitesimal quantities. Here the term with ϵ_0 characterizes the lateral motion of the cylinder from the center of the vortex, while the term with ϵ_1 characterizes the inclination of the cylinder from the z axis. The pressure p on the cylinder is obtained by evaluating Eq. (7) on this displaced surface

$$p = \rho_l a\Omega^2(\epsilon_0' + \epsilon_1' z) - i\rho_l(\Omega + \omega)\Phi', \tag{9}$$

where we define

$$\epsilon_0' \equiv \epsilon_0 e^{-i\varphi}e^{-i\omega t}, \quad \epsilon_1' \equiv \epsilon_1 e^{-i\varphi}e^{-i\omega t}.$$

The hydrodynamic force on the cylinder is

$$\vec{F} = -\int p\hat{n}\, dS, \tag{10}$$

where the integral is originally taken over the displaced surface. Since Eq. (9) is already of first order in the small quantities, however, the integral can instead be evaluated on the unperturbed

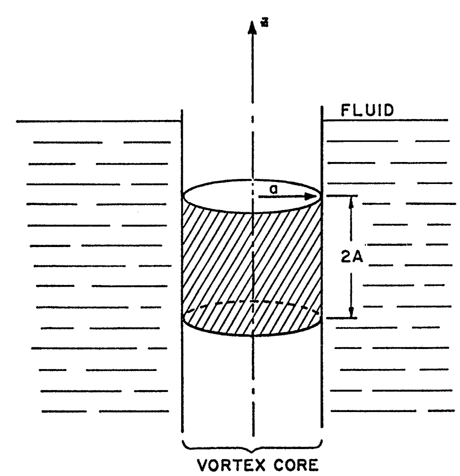

FIG. 1. Geometry of the cylinder in the vortex core.

surface of the cylinder with $\hat{n}(=\hat{x}\cos\varphi+\hat{y}\sin\varphi)$ the unit vector normal to the z axis. In this way, Eqs. (9) and (10) give the x and y components of the force:

$$F_x=iF_y=-\pi a\rho_l\left(2\Omega^2 aA\epsilon_0-i(\Omega+\omega)\int_{-A}^{A}dz\chi(a,z)\right)e^{-i\omega t}, \tag{11a}$$

with the corresponding radial component

$$F_r=F_x\cos\varphi+F_y\sin\varphi=F_x e^{-i\varphi}. \tag{11b}$$

Here, the function χ is defined by $\Phi'=\chi(r,z)e^{-i\varphi}\times e^{-i\omega t}$. The calculation of the torque $\vec{\tau}$ is very similar and yields

$$\tau_x=i\tau_y=-i\,\pi a\rho_l\left(\tfrac{2}{3}\Omega^2A^3a\,\epsilon_1-i(\Omega+\omega)\times\int_{-A}^{A}z\,dz\,\chi(a,z)\right)e^{-i\omega t}, \tag{12a}$$

$$\tau_r=\tau_x\cos\varphi+\tau_y\sin\varphi=\tau_x e^{-i\varphi}. \tag{12b}$$

Newton's second law determines the motion of the cylinder through the relations

$$F_x=-M\omega^2\epsilon_0 e^{-i\omega t},\quad F_y=iM\omega^2\epsilon_0 e^{-i\omega t},$$
$$\tau_x=-iI\omega^2\epsilon_1 e^{-i\omega t},\quad \tau_y=-I\omega^2\epsilon_1 e^{-i\omega t},$$

where $I=(\frac{1}{4}a^2+\frac{1}{3}A^2)M$ is the moment of inertia of the cylinder about an axis perpendicular to the z axis. These equations can be combined to give

$$F_r=-M\omega^2\epsilon_0', \tag{13a}$$

$$\tau_r=-iI\omega^2\epsilon_1'. \tag{13b}$$

When Eqs. (11) and (12) are substituted into (13a) and (13b), the resulting expressions can be solved for ϵ_0 and ϵ_1:

$$\epsilon_0=-i\,\frac{\pi a\rho_l}{V}\left(\frac{\omega+\Omega}{M\omega^2/V-\rho_l\Omega^2}\right)\int_{-A}^{A}dz\,\chi(a,z), \tag{14}$$

$$\epsilon_1=-i\,\frac{\pi a\rho_l}{V}\left(\frac{\omega+\Omega}{I\omega^2/V-\frac{1}{3}A^2\rho_l\Omega^2}\right)\int_{-A}^{A}z\,dz\,\chi(a,z), \tag{15}$$

where $V=2\pi a^2A$ is the volume of the cylinder. Note that ϵ_0 and ϵ_1 vanish in the limit of a fixed cylinder ($M\to\infty$).

The remaining step in our formulation is the determination of the velocity potential χ. For $|z|>A$, it is clear that χ satisfies the free-surface boundary condition[2,7]

$$\frac{\partial\chi}{\partial r}=\nu\chi\quad\text{for } r=a,\ |z|>A, \tag{16}$$

where

$$\nu\equiv-\frac{1}{a}\left(1+\frac{\omega}{\Omega}\right)^2=-\frac{1}{a}\left(1+\frac{kaK_0(ka)}{K_1(ka)}\right)$$

is appropriate for the wave with $l=-1$. In the region $|z|<A$ occupied by the cylinder, the liquid must remain in contact with the surface, whose normal component of velocity can be obtained from Eq. (8) as $-i\omega(\epsilon_0'+\epsilon_1'z)$. If $\hat{n}$ denotes the normal to the *displaced* surface, we therefore obtain the boundary condition $-i\omega(\epsilon_0+\epsilon_1z)=(\vec{v}_0-\vec{\nabla}\Phi')\cdot\hat{n}$. A straightforward calculation to lowest order in the small quantities yields

$$\frac{\partial\chi}{\partial r}=i(\omega+\Omega)(\epsilon_0+\epsilon_1z)\quad\text{for } r=a,\ |z|<A. \tag{17}$$

Since $\chi e^{-i\varphi}$ satisfies Laplace's equation, and χ must remain bounded for $r\to\infty$, the boundary conditions (14)–(17) complete the specification of our problem.

The scattering calculation can be simplified with a Green's function satisfying the free-surface boundary condition

$$\nabla^2G(\vec{R},\vec{R}')=-\delta(\vec{R}-\vec{R}')\quad\text{for } r,r'>a,\ -\infty<z,z'<\infty, \tag{18a}$$

$$\frac{\partial G(\vec{R},\vec{R}')}{\partial r'}=\nu G(\vec{R},\vec{R}')\quad\text{for } r'=a, \tag{18b}$$

where $\vec{R}$, $\vec{R}'$ denote three-dimensional coordinate vectors. We need retain only the part with the polar angle dependence $e^{-i(\varphi-\varphi')}$, and a simple analysis leads to

$$G(r,z;r',z')=\frac{1}{\pi}\int_0^\infty dq\cos q(z-z')G(q,r,r'), \tag{19a}$$

where

$$G(q,r,r')=K_1(qr_>)\left(I_1(qr_<)-\frac{qI_1'(qa)-\nu I_1(qa)}{qK_1'(qa)-\nu K_1(qa)+i\epsilon}K_1(qr_<)\right). \tag{19b}$$

Here $r_>$ and $r_<$ are the larger and smaller of r and r', I_1 is the modified Bessel function of the first kind,[8] and the small imaginary term $i\epsilon$ ensures the outgoing wave condition.

Our main interest is the reflection and transmission probability, which requires the form of the Green's function for $|z-z'|\to\infty$. If the integration path in Eq. (19a) is deformed from the real to the imaginary axis, a detailed calculation gives

$$\begin{aligned}G(r,z;r',z')=&\left[8\sqrt{2}\,(rr')^{1/2}u^{3/2}\right]^{-1}{}_2F_1(\tfrac{5}{4},\tfrac{3}{4};2;u^{-2})\\&+iCa^{-1}e^{ik|z-z'|}K_1(kr)K_1(kr')\\&-\frac{1}{4}\int_0^\infty dq\,e^{-q|z-z'|}\left[qa\,J_0(qa)+(\nu a+1)J_1(qa)\right]\\&\times\left(\frac{H_1^{(2)}(qr)H_1^{(2)}(qr')}{qaH_0^{(2)}(qa)+(\nu a+1)H_1^{(2)}(qa)}+\frac{H_1^{(1)}(qr)H_1^{(1)}(qr')}{qaH_0^{(1)}(qa)+(\nu a+1)H_1^{(1)}(qa)}\right).\end{aligned} \tag{20}$$

Here

$$u=(2rr')^{-1}\left[(z-z')^2+r^2+r'^2\right],$$

$J_i, H_i^{(1)}$ and $H_i^{(2)}$ are Bessel functions and Hankel functions, respectively,[8] ${}_2F_1$ is the hypergeometric function,[8] and C is a dimensionless quantity defined by

$$C^{-1}=ka\left[K_0(ka)\right]^2-ka\left[K_1(ka)\right]^2+2K_0(ka)K_1(ka).$$

This form of G is very convenient because the asymptotic behavior for $|z-z'|\to\infty$ can be determined by inspection to be

$$G(r,z;r',z')\sim iCa^{-1}e^{ik|z-z'|}K_1(kr)K_1(kr')\,,\qquad |z-z'|\to\infty. \tag{21}$$

Green's theorem now allows us to formulate an integral equation for the velocity potential $\chi(r,z)$

$$\chi(r,z)=\chi_{\rm inc}(r,z)+\int\frac{dS'}{2\pi}\left(\chi(r',z')\frac{\partial G(r,z;r',z')}{\partial r'}-G(r,z;r',z')\frac{\partial\chi(r',z')}{\partial r'}\right)\,, \tag{22}$$

where G is given in Eq. (19) and the integral is taken over the surface of the cylinder in contact with the liquid. In accordance with the scattering boundary conditions, we have added the incident wave $\chi_{\rm inc}=\chi_0\,e^{ikz}K_1(kr)$, which satisfies the $l=-1$ projection of Laplace's equation with the free-surface boundary condition. It is convenient to separate Eq. (22) into symmetric and antisymmetric parts:

$$\chi(r,z)=\chi_s(r,z)+\chi_a(r,z),$$

where

$$\chi_s(r,-z)=\chi_s(r,z)\quad\text{and}\quad\chi_a(r,-z)=-\chi_a(r,z).$$

For the symmetric (antisymmetric) case, the ϵ_1 (ϵ_0) term of Eq. (17) vanishes. Thus the symmetric and antisymmetric parts satisfy the integral equations

$$\chi_s(r,z)=\chi_0\cos kzK_1(kr)+\int_{-A}^{A}dz'a\,G(r,z;a,z')\times[\nu\chi_s(a,z')-i(\omega+\Omega)\epsilon_0], \tag{23}$$

$$\chi_a(r,z)=i\,\chi_0\sin kzK_1(kr)+\int_{-A}^{A}dz'a\,G(r,z;a,z')\times[\nu\chi_a(a,z')-i(\omega+\Omega)\epsilon_1z'], \tag{24}$$

where the boundary conditions (16), (17), and (18b) have been used to simplify the integrand. For large $|z|$, Eq. (23) approaches the asymptotic limit

$$\chi_s(r,z)\sim\begin{cases}(A_se^{-ikz}+B_se^{ikz})K_1(kr), & z\to\infty\\(A_se^{ikz}+B_se^{-ikz})K_1(kr), & z\to-\infty\end{cases} \tag{25a}$$

where

$$A_s=\tfrac12\chi_0,$$

$$B_s=\tfrac12\chi_0+iCK_1(ka)\int_{-A}^{A}dz'\cos kz'\times[\nu\chi_s(a,z')-i(\omega+\Omega)\epsilon_0]. \tag{25b}$$

Similarly, the antisymmetric part becomes

$$\chi_a(r,z)\sim\begin{cases}(A_ae^{-ikz}+B_ae^{ikz})K_1(kr), & z\to\infty\\-(A_ae^{ikz}+B_ae^{-ikz})K_1(kr), & z\to-\infty\end{cases} \tag{26a}$$

where

$$A_a=-\tfrac12\chi_0\,,$$

$$B_a=\tfrac12\chi_0+CK_1(ka)\int_{-A}^{A}dz'\sin kz'\times[\nu\chi_a(a,z')-i(\omega+\Omega)z'\epsilon_1]. \tag{26b}$$

The actual solution χ for a wave incident from $z=-\infty$ is the sum of the symmetric and antisymmetric parts, and we find

$$\chi(r,z)=\chi_s(r,z)+\chi_a(r,z)\sim\begin{cases}(B_s+B_a)\,e^{ikz}K_1(kr), & z\to\infty\\ [\chi_0e^{ikz}+(B_s-B_a)\,e^{-ikz}]K_1(kr)\,, & z\to-\infty.\end{cases} \tag{27}$$

Consequently, the reflection and transmission amplitudes are given by

$$R=\chi_0^{-1}(B_s-B_a),\quad T=\chi_0^{-1}(B_s+B_a). \tag{28}$$

From the above expressions, it is evident that the function χ is needed only in the restricted range $r=a$, $|z|<A$, which allows us to simplify the calculation. Apply the operator $\partial/\partial r$ to both sides of Eqs. (23) and (24), and then set $r=a$ with $|z|<A$. The integrand can be rewritten with the relation

$$\left(\frac{\partial}{\partial r}G(r,z;a,z')\right)_{r=a}=-(1/a)\delta(z-z')+\nu G(a,z;a,z')\,, \tag{29}$$

which can be proved from the integral representation (19). Thus we obtain

$$\chi_s(a,z)=k\nu^{-1}\chi_0\cos(kz)K_1'(ka)+\int_{-A}^{A}dz'a\,G(a,z;a,z')\times[\nu\chi_s(a,z')-i(\omega+\Omega)\epsilon_0], \tag{30}$$

$$\chi_a(a,z)=ik\nu^{-1}\chi_0\sin(kz)K_1'(ka)+\int_{-A}^{A}dz'a\,G(a,z;a,z')$$

$$\times[\nu\chi_a(a, z') - i(\omega+\Omega)z'\epsilon_1]. \tag{31}$$

It is helpful to introduce dimensionless quantities

$$\chi(\xi) = \chi(a, z)/\chi_0, \quad \xi = z/A, \quad \xi' = z'/A,$$

$$\kappa = ka, \quad \alpha = A/a, \quad \nu_0 = \nu A,$$

$$\mu_0 = \rho_l(\omega+\Omega)^2/[M\omega^2/V - \rho_l\Omega^2].$$

With these new variables, Eqs. (30) and (31) reduce to

$$\chi_s(\xi) = K_1(\kappa)\cos\alpha\kappa\xi + \nu_0\int_{-1}^{1} d\xi' G(\xi, \xi')\chi_s(\xi')$$

$$-\tfrac{1}{2}\alpha\mu_0\int_{-1}^{1} d\xi' G(\xi, \xi')\int_{-1}^{1} d\xi''\chi_s(\xi'') , \tag{32}$$

$$\chi_a(\xi) = iK_1(\kappa)\sin\alpha\kappa\xi + \nu_0\int_{-1}^{1} d\xi' G(\xi, \xi')\chi_a(\xi')$$

$$-\tfrac{3}{2}\alpha\mu_0\int_{-1}^{1} d\xi'\xi' G(\xi, \xi')\int_{-1}^{1} d\xi''\xi''\chi_a(\xi''), \tag{33}$$

where we have used the identity $\alpha\kappa K_1'(\kappa) = \nu_0 K_1(\kappa)$. The factor $G(\xi, \xi')$ can be obtained directly from Eq. (19):

$$G(\xi, \xi') \equiv aG(a, z; a, z')$$

$$= \frac{1}{\pi}\int_0^\infty d\eta \frac{\cos\alpha\eta(\xi-\xi')}{F(\eta) - F(\kappa) - i\epsilon}$$

$$= ie^{i\alpha\kappa|\xi-\xi'|}C[K_1(\kappa)]^2 + \pi^{-1}\int_0^\infty d\eta e^{-\alpha\eta|\xi-\xi'|}P(\eta, \kappa), \tag{34}$$

where the second line is derived with the relation

$$K_1(\eta)I_1'(\eta) - I_1(\eta)K_1'(\eta) = \eta^{-1}.$$

Here we have introduced the abbreviations

$$F(x) = \frac{xK_0(x)}{K_1(x)},$$

$$P(\eta, \kappa) = \frac{2/\pi}{[\eta J_0(\eta) + F(\kappa)J_1(\eta)]^2 + [\eta Y_0(\eta) + F(\kappa)Y_1(\eta)]^2}$$

The reflection and transmission amplitudes can also be written in dimensionless form:

$$R = \mathcal{S} - \mathcal{A}, \quad T = 1 + \mathcal{S} + \mathcal{A}, \tag{35}$$

with

$$\mathcal{S} = i\nu_0 CK_1(\kappa)\int_{-1}^{1}\chi_s(\xi)\cos\alpha\kappa\xi\, d\xi$$

$$-i\alpha C\mu_0 K_1(\kappa)\frac{\sin\alpha\kappa}{\alpha\kappa}\int_{-1}^{1}\chi_s(\xi)d\xi, \tag{36a}$$

$$\mathcal{A} = \nu_0 CK_1(\kappa)\int_{-1}^{1}\chi_a(\xi)\sin\alpha\kappa\xi\, d\xi$$

$$-3\alpha C\mu_0 K_1(\kappa)\frac{\sin\alpha\kappa - \alpha\kappa\cos\alpha\kappa}{(\alpha\kappa)^2}\int_{-1}^{1}\chi_a(\xi)\xi\, d\xi, \tag{36b}$$

where the explicit forms of ϵ_0 and ϵ_1 [Eqs. (14) and (15)] have been used. Finally, it is interesting to evaluate the ratio of the radial amplitude of the cylinder ϵ_0 to that of the incident wave, which is given by

$$\sigma \equiv \frac{i(\omega+\Omega)\epsilon_0}{k\chi_0 K_1'(ka)} = \frac{\alpha\mu_0}{2\nu_0 K_1(\kappa)}\int_{-1}^{1} d\xi\,\chi_s(\xi) . \tag{37}$$

III. APPROXIMATE SOLUTION

Our basic problem has now been reduced to the linear integral equations (32) and (33). Unfortunately, it is not possible to solve them exactly, and we therefore rely on approximation schemes. In a previous study of a dock on a semi-infinite sea,[5] the solutions were expanded in Fourier series. Although a similar approach is possible here, the first-order approximation has the unphysical feature of perfect transmission at $kA = \pi$, 2π, ..., which is precisely the important range of wavelengths for an ion in He II. Furthermore, higher-order approximations become very complicated and do not seem useful. Hence we instead derive an explicit solution for long and short wavelengths and make a simple interpolation between the two limits. As shown below, this rather crude procedure works well in practice.

Consider the long-wavelength limit ($\kappa \to 0$), when the dimensionless Green's function (34) can be approximated as ($\gamma \approx 0.577$ is Euler's constant)

$$G(\xi, \xi') \approx iC[K_1(\kappa)]^2 e^{i\alpha\kappa|\xi-\xi'|}$$

$$+\frac{1}{2}\int_0^\infty d\eta \frac{\eta^2 e^{-\alpha\eta|\xi-\xi'|}}{\{\eta^2[\ln(2/\eta)-\gamma] + \kappa^2[\ln(2/\kappa)-\gamma]\}^2 + (\frac{1}{2}\pi\eta^2)^2}$$

$$\approx \frac{i}{2\kappa[\ln(2/\kappa) - \gamma - \frac{1}{2}]}$$

$$+\frac{1}{2\kappa}\int_0^\infty dx \frac{x^2}{\{x^2[\ln(2/\kappa x)-\gamma] + \ln(2/\kappa)-\gamma\}^2 + (\frac{1}{2}\pi x^2)^2} . \tag{38}$$

The dominant contribution to the integral arises from the region $x \approx 1$. In the limit $\kappa \to 0$, it follows that the denominator may be approximated as $[\ln(2/\kappa)-\gamma]^2(x^2+1)^2$, and Eq. (38) takes the form

$$G(\xi, \xi') \approx \frac{i}{2\kappa[\ln(2/\kappa) - \gamma - \frac{1}{2}]} + \frac{\pi}{8\kappa[\ln(2/\kappa)-\gamma]^2}$$

$$\approx \frac{i}{2\kappa[\ln(2/\kappa)-\gamma]}\left[1 + O\!\left(\frac{1}{\ln(1/\kappa)}\right)\right] . \tag{39}$$

We now expand Eq. (32) and (33) for small κ:

$$\chi_s(\xi) \approx \frac{1}{\kappa} + \frac{i(\nu_0 - \alpha\mu_0)}{2\kappa[\ln(2/\kappa)-\gamma]}\int_{-1}^{1} d\xi'\chi_s(\xi'), \tag{40a}$$

$$\chi_a(\xi) = O(1) . \tag{40b}$$

In the same limit, it is easily verified that the factor $\nu_0 - \alpha\mu_0$ reduces to

$$\nu_0 - \alpha\mu_0 \approx \alpha \frac{M}{V\rho_l}\left(\frac{\omega}{\Omega}\right)^2 \approx \tfrac{1}{4}\alpha \frac{M}{V\rho_l}\kappa^4[\ln(2/\kappa)-\gamma]^2 , \tag{41}$$

and Eq. (40a) becomes

$$\chi_s(\xi) \approx \frac{1}{\kappa} + \frac{i\alpha}{8}\frac{M}{V\rho_l}\kappa^3[\ln(2/\kappa)-\gamma]\int_{-1}^{1} d\xi'\chi_s(\xi') . \tag{42}$$

Integrate Eq. (42) from -1 to 1; the result may be solved to give

$$\int_{-1}^{1} d\xi\, \chi_s(\xi) \approx \frac{2}{\kappa}\left(1 - \frac{i\alpha}{4}\frac{M}{V\rho_l}\kappa^3[\ln(2/\kappa)-\gamma]\right)^{-1} \approx \frac{2}{\kappa} , \tag{43a}$$

while

$$\int_{-1}^{1} d\xi\, \xi\chi_a(\xi) = O(1) . \tag{43b}$$

These expressions allow us to evaluate $\mathcal{S}$ and $\mathcal{A}$ [Eqs. (36)] explicitly in the long-wavelength limit

$$\mathcal{S} \approx \tfrac{1}{4} i\alpha(M/V\rho_l)\kappa^3[\ln(2/\kappa)-\gamma] ,$$
$$\mathcal{A} = O\{\kappa^5[\ln(2/\kappa)-\gamma]\} . \tag{44}$$

Consequently, the reflection amplitude becomes

$$R \approx \tfrac{1}{4} i\alpha(M/V\rho_l)\kappa^3[\ln(2/\kappa)-\gamma] , \tag{45}$$

with the corresponding reflection probability

$$|R|^2 = \left(\frac{M}{8\pi a^3\rho_l}\right)^2 \kappa^6[\ln(2/\kappa)-\gamma]^2 , \tag{46}$$

where we have used the relation $V = 2\pi a^2 A$. In the long-wavelength limit, it is notable that $|R|^2$ is independent of the length A of the cylinder, depending only on the effective mass M of the ion and the core radius a. This result can also be derived with the truncation procedure used in Ref. 5.

The relative radial amplitude of the cylinder (37) is easily calculated for $\kappa \to 0$ and yields

$$\sigma \approx 1 , \quad \kappa \to 0 . \tag{47}$$

Thus the cylinder moves with the fluid, as is usual for the surface waves on a sea or channel.

The short-wavelength limit is studied in the Appendix, where $|R|^2$ is shown to have the expected behavior

$$|R|^2 \sim 1 , \quad \kappa \to \infty. \tag{48}$$

Since $|R|^2$ is known in both limits ($\kappa \ll 1$ and $\kappa \gg 1$), it is natural to suggest the interpolation formula

$$|R|^2 = H^2/(1+H^2) , \tag{49}$$

where

$$H \equiv (M/8\pi a^3\rho_l)\kappa^3[\ln(2/\kappa)-\gamma] = (Mk^3/8\pi\rho_l)[\ln(2/ka)-\gamma] . \tag{50}$$

Apart from the logarithmic dependence on the core radius a, the resulting approximate $|R|^2$ depends only on the model-independent parameters M, k, and ρ_l.

An ion moving along a vortex line experiences a drag force owing to collisions with the thermally excited vortex waves. This effect reduces the mobility μ of a trapped ion relative to that of a free one. We shall compute the drag force in terms of the reflection probability, which leads to the expression[9]

$$\frac{1}{\mu} = -\frac{2\hbar}{\pi e}\int_0^\infty dk\, k^2 \frac{\partial n}{\partial k}\, |R(k)|^2 , \tag{51}$$

where e is the charge on the cylinder, $|R(k)|^2$ is the reflection probability in the rest frame of the ion, and $n(k)$ is the Bose-Einstein distribution for the vortex waves. The same expression remains valid if the thermal motion of the ion is taken into account with a Boltzmann distribution.

IV. RESULTS AND DISCUSSION

Figure 2 shows our approximate reflection probability $|R|^2$ for $a = 1$ Å and various values of M, together with that of Douglass.[2] Note that Eq. (49) has a spurious zero at $ka \approx 1$, which fortunately lies well above the range of thermal wavelengths for vortex waves in He II. For the same reason, any possible resonant behavior at $\omega \approx \Omega(\rho_l V/M)^{1/2}$ [arising from the factor μ_0 in Eqs. (32) and (33)] is irrelevant for He II, where $\hbar\Omega/k_B \approx 10$ °K.

The reflection probability in Fig. 2 was used to evaluate the temperature-dependent mobility [Eq. (51)] for $a = 1$ Å, with the results indicated in Fig. 3. We see that the lightest effective mass

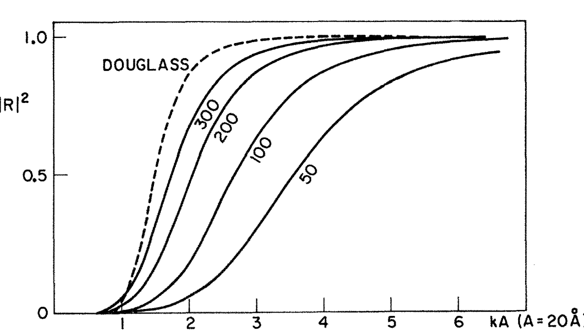

FIG. 2. Approximate reflection probability [Eq. (49)] for $a = 1$ Å and various effective masses ($50\, m_{He} \le M \le 300 m_{He}$), together with Douglass's numerical curve for $A = 20$ Å. Curves are labeled with the value of M/m_{He}.

leads to the largest mobility, as is plausible from physical considerations. The experimental curve[1,2] is also shown for comparison. At low temperatures ($T \lesssim 1\,^\circ\mathrm{K}$), the vortex waves clearly make an important contribution to the drag force on the trapped ion and must be included in any complete theory. At higher temperatures, however, the observed mobility decreases more rapidly than predicted here, owing to the enhanced roton density.[3]

The mobility is quite sensitive to the parameters M and a, as is illustrated in Fig. 4. For a given effective mass, the mobility decreases rapidly as a increases. In particular, the reasonable values $M \approx 100 m_{\mathrm{He}}$ and $a \approx 1$ Å provide an acceptable fit to the experiments at low temperature.

The present approximate calculation has been restricted to the drag force on a moving trapped ion arising from the scattering of vortex waves previously present. The creation of more vortex waves can lead to an additional drag force, which we hope to examine in a subsequent paper.

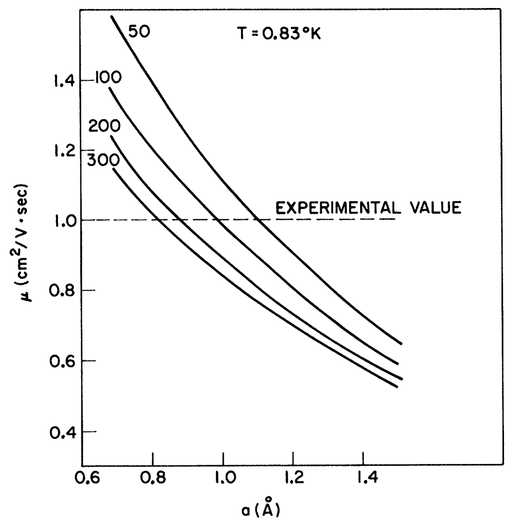

FIG. 4. Predicted mobility at $T = 0.83\,^\circ\mathrm{K}$ as a function of the core radius a for various effective masses. The experimental value is $\mu_{\mathrm{expt}} \approx 1\,\mathrm{cm}^2/\mathrm{V\,sec}$. The curves are labeled with the value of M/m_{He}.

APPENDIX

We here consider the problem of short wavelengths, and, for simplicity, treat only a fixed cylinder ($M \to \infty$). The basic integral equation for $\chi = \chi_s + \chi_a$ is

$$\chi(\xi) = K_1(\kappa) e^{i\alpha\kappa\xi} + \nu_0 \int_{-1}^{1} d\xi' G(\xi, \xi') \chi(\xi'). \tag{A1}$$

In the limit $\alpha\kappa |\xi - \xi'| \to \infty$, we need only the first term of Eq. (34), which reduces to the asymptotic form $G(\xi, \xi') \sim i e^{i\alpha\kappa|\xi - \xi'|}$ as $\kappa \to \infty$. In the separate regions $\xi > 1$ and $\xi < -1$, the asymptotic solution becomes

$$\chi^{>}(\xi) \sim K_1(\kappa) e^{i\alpha\kappa\xi} + i\nu_0 A(1) e^{i\alpha\kappa\xi}\ , \quad \xi > 1 \tag{A2a}$$

$$\chi^{<}(\xi) \sim K_1(\kappa) e^{i\alpha\kappa\xi} + i\nu_0 B(-1) e^{-i\alpha\kappa\xi}, \quad \xi < -1 \tag{A2b}$$

where

$$A(\xi) = \int_{-1}^{\xi} e^{-i\alpha\kappa\xi'} \chi(\xi') d\xi',$$
$$B(\xi) = \int_{\xi}^{1} e^{i\alpha\kappa\xi'} \chi(\xi') d\xi'. \tag{A3}$$

Similarly, the wave for $|\xi| < 1$ can be written

$$\chi(\xi) = K_1(\kappa) e^{i\alpha\kappa\xi} + i\nu_0 e^{i\alpha\kappa\xi} A(\xi) + i\nu_0 e^{-i\alpha\kappa\xi} B(\xi). \tag{A4}$$

Differentiate Eq. (A3) with respect to ξ. A combination with Eq. (A4) gives a pair of coupled equations for A and B:

$$\frac{dA(\xi)}{d\xi} = K_1(\kappa) + i\nu_0 A(\xi) + i\nu_0 e^{-2i\alpha\kappa\xi} B(\xi),$$
$$\frac{dB(\xi)}{d\xi} = -K_1(\kappa) e^{2i\alpha\kappa\xi} - i\nu_0 e^{2i\alpha\kappa\xi} A(\xi) - i\nu_0 B(\xi). \tag{A5}$$

Eliminating $B(\xi)$ from the above equations, we derive

$$\frac{d^2 A(\xi)}{d\xi^2} + 2i\alpha\kappa \frac{dA(\xi)}{d\xi} + 2\alpha\kappa\nu_0 A(\xi) = 2i\alpha\kappa K_1(\kappa). \tag{A6}$$

This ordinary differential equation can be solved to give

$$A(\xi) = c_1 e^{-i\lambda_1\xi} e^{i\lambda_2\xi} + c_2 e^{-i\lambda_1\xi} e^{-i\lambda_2\xi} + iK_1(\kappa)/\nu_0\,, \tag{A7}$$

where

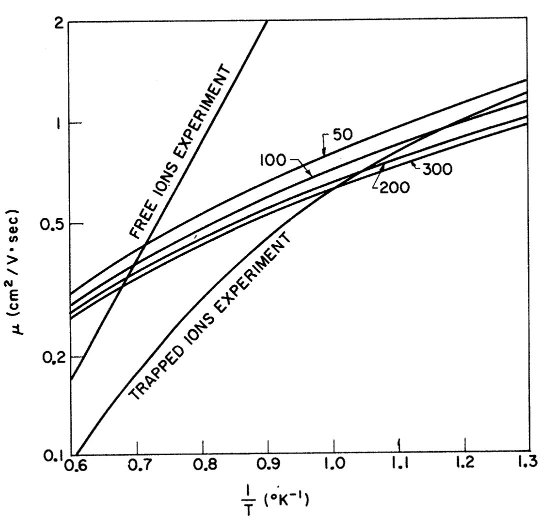

FIG. 3. Temperature-dependent mobility [Eq. (51)] evaluated with Eq. (49), where $a = 1$ Å and M takes various values. Curves are labeled with the value of M/m_{He}.

$$\lambda_1 = \alpha\kappa\ , \quad \lambda_2 = (\alpha^2\kappa^2 + 2\alpha\kappa\nu_0)^{1/2}. \tag{A8}$$

The constants c_1 and c_2 must be chosen to satisfy the boundary conditions $A(-1) = B(1) = 0$, which yields

$$A(\xi) = \frac{iK_1(\kappa)}{\nu_0} - \frac{iK_1(\kappa)}{\nu_0} e^{-i\lambda_1(1+\xi)} \times \frac{e^{i\lambda_2(1-\xi)}(\lambda_1 + \nu_0 - \lambda_2) - e^{-i\lambda_2(1-\xi)}(\lambda_1 + \nu_0 + \lambda_2)}{e^{2i\lambda_2}(\lambda_1 + \nu_0 - \lambda_2) - e^{-2i\lambda_2}(\lambda_1 + \nu_0 + \lambda_2)}\ , \tag{A9a}$$

$$B(\xi) = \frac{iK_1(\kappa)[e^{i(\xi-1)(\lambda_1-\lambda_2)} - e^{i(\xi-1)(\lambda_1+\lambda_2)}]}{e^{2i\lambda_2}(\lambda_1 + \nu_0 - \lambda_2) - e^{-2i\lambda_2}(\lambda_1 + \nu_0 + \lambda_2)}\ . \tag{A9b}$$

Equation (A2) shows that the quantities of physical interest are $A(1)$ and $B(-1)$. In short-wavelength limit, we find

$$\left.\begin{aligned} A(1) &\approx i\nu_0^{-1}K_1(\kappa), \\ B(-1) &\approx -\nu_0^{-1}K_1(\kappa)e^{-2i\alpha\kappa}\ , \end{aligned}\right\} \kappa \to \infty \tag{A10}$$

with the corresponding transmission and reflection amplitudes

$$\left.\begin{aligned} T &= \frac{K_1(\kappa) + i\nu_0 A(1)}{K_1(\kappa)} \approx 0\ , \\ R &= \frac{i\nu_0 B(-1)}{K_1(\kappa)} \approx -ie^{-2i\alpha\kappa}\ , \end{aligned}\right\} \kappa \to \infty\ . \tag{A11}$$

Thus $|T|^2 \to 0$ and $|R|^2 \to 1$ as $\kappa \to \infty$, which proves the assertion in Sec. III.

---

†Research sponsored by Contract No. F44620-68-C-0075.

*Alfred P. Sloan Foundation Fellow.

[1]W. I. Glaberson, D. M. Strayer, and R. J. Donnelly, Phys. Rev. Letters 20, 1428 (1968).

[2]R. L. Douglass, Phys. Rev. 174, 255 (1968).

[3]W. I. Glaberson, D. M. Strayer, and R. J. Donnelly, Phys. Rev. Letters 21, 1740 (1968).

[4]H. Levine, J. Math. Phys. 6, 1231 (1965).

[5]A. L. Fetter, Phys. Fluids 12, 741 (1969).

[6]H. Lamb, *Hydrodynamics* (Dover, New York, 1945), 6th ed., Chaps. III and IX.

[7]A. L. Fetter, in *Lectures in Theoretical Physics*, edited by K. T. Mahanthappa and W. E. Brittin (Gordon and Breach, New York, 1969), Vol. XI-B, p. 321.

[8]*Handbook of Mathematical Functions with Formulas, Graphs, and Mathematical Tables*, edited by M. Abramowitz and I. A. Stegun (U. S. Department of Commerce, National Bureau of Standards, Washington, D. C., 1968), Appl. Math. Ser. 55, Chaps. 9 and 15.

[9]G. Baym, R. G. Barrera, and C. J. Pethick, Phys. Rev. Letters 22, 20 (1969).

PHYSICAL REVIEW A VOLUME 2, NUMBER 5 NOVEMBER 1970

Multimode Effects in Intensity Correlation Measurements

H. P. Weber and H. G. Danielmeyer

Bell Telephone Laboratories, Incorporated, Holmdel, New Jersey 07733

(Received 21 May 1970)

Intensity correlation measurements of lasers oscillating in many transverse modes are found to be very sensitive to slight misalignment of the beams that have to be superimposed on each other for such measurements. This fact is shown to be due to the lack of spatial coherence in such lasers. It is theoretically shown that if the modes oscillate independently of each other, the fluctuation behavior becomes different for different points of the beam profile. This fact is demonstrated experimentally. An analysis of intensity correlation measurements of mode-locked lasers oscillating in many transverse modes is presented. The effects of slight misalignments on measurements of contrast ratios in two-photon fluorescence (TPF) patterns and second-harmonic measurements are discussed. In TPF measurements, even minute misalignments effectively reduce the contrast ratio from 3:1 to 2:1. Previously published data may be explained in this way.

INTRODUCTION

Intensity correlation measurements have recently become a popular means of obtaining information about the time behavior of laser light signals in times shorter than the resolution time of electronic detection systems. Such measurements make use of optical nonlinear response characteristics. In one case, the second-order intensity correlation function[1] $G^{(2)}(\tau)$ defined as

$$G^{(2)}(\tau) = \langle I(t)I(t+\tau)\rangle \tag{1}$$

is directly measured by a process involving second-harmonic generation.[2-4] In a further method[5] involving two-photon absorption-induced fluorescence (TPF) the intensity correlation is superimposed on a constant background. One measures[6-8]